Conformations of Cyclic Octapeptides. 5. Crystal Structure of Cyclo(Cys-Gly-Pro-Phe)$_2$ and Rotating Frame Relaxation ($T_{1\rho}$) NMR Studies of Internal Mobility in Cyclic Octapeptides

Kenneth D. Kopple,* Yu-Sen Wang,† Anita Go Cheng,† and Krishna K. Bhandary‡

Contribution from the Department of Chemistry, Illinois Institute of Technology, Chicago, Illinois 60616, and the Biophysics Department, Roswell Park Memorial Institute, Buffalo, New York 14263. *Received September 17, 1987*

Abstract: The disulfide-bridged cyclic octapeptide cyclo(Cys-Gly-Pro-Phe)$_2$ (I) was synthesized, a crystal structure was determined, and studies of proton spin–lattice relaxation in the rotating frame were made to probe its internal mobility in solution. Cyclo(Cys-Gly-Pro-Phe)$_2$ crystallized from methanol in the monoclinic unit cell, space group $P2_1$, with dimensions a = 10.164 (6) Å, b = 13.610 (1) Å, c = 15.702 (3) Å, and β = 101.12 (3)°. The asymmetric unit contains one octapeptide molecule and four water molecules. The peptide backbone contains Pro-Phe β-turns, bears a strong resemblance to the backbone of β-amanitin, and is roughly similar to backbones previously reported for cyclo(Ala-Gly-Pro-Phe)$_2$ diastereomers. It is asymmetric, with one type I and one type II turn, different side chain rotamers at the two Cys residues, and different orientations of the two Cys-Gly peptide bond planes relative to the peptide ring. The NMR spectrum of cyclo(Cys-Gly-Pro-Phe)$_2$ in dimethyl sulfoxide or dimethyl sulfoxide–chloroform solution at 55 °C is averaged to apparent C_2 symmetry and is similar to that of cyclo(Ala-Gly-Pro-Phe)$_2$ (II) at room temperature. For both peptides, proton $T_{1\rho}$ measurements were made as a function of spin-locking field and temperature. An approximate analysis of the NMR relaxation data and observation of differential line broadening at lower temperatures suggest that an intramolecular motion averaging the conformations at the cystine bridge and the Cys-Gly peptide bond has a barrier near 7 kcal/mol and that rotation of the Pro-Phe amide plane to interchange type I and II Pro-Phe turns has a lower barrier. The range of applicability of proton $T_{1\rho}$ measurements to study peptide conformational exchange and the use of a two-site approximation for analysis of $T_{1\rho}$ data are discussed. Results for I, II, and two diastereomers of II are compared.

Peptides are conformationally mobile molecules, and the internal motions of peptide chains can have characteristic times ranging from minutes to picoseconds. Solution NMR studies usually report conformational exchange rates that are of the order of the chemical shift differences, 10^3 s^{-1} or slower, or those motions that are near the Larmor frequencies of the observed nuclei, 10^9–10^{10} s^{-1}. Internal motions between 10^3 and 10^9 s^{-1} in solution are not readily examined by the usual solution NMR methods.

Although proton or ^{13}C magnetic resonance spectra are narrow-line averages over the exchanging species for conformation interchanges occurring faster than 10^4 s^{-1}, chemical shift fluctuations at this rate or above can contribute significantly to the rate of spin–lattice relaxation in the rotating frame, $1/T_{1\rho}$.[1,2] We have been exploring the potential of proton $T_{1\rho}$ measurements as a reporter of peptide internal mobility.

The chemical exchange contribution to the $T_{1\rho}$ relaxation of a given nuclear spin is determined by the exchange rates and the chemical shift differences between sites.[1] For a given exchange rate, larger chemical shift fluctuations have larger effects. Because chemical shift fluctuations have a maximal effect at the frequency of precession about the spin-locking field, the exchange contribution can be dependent on the strength of that field. For exploratory purposes, a two-site exchange model may be applied to the field dependence to extract a characteristic exchange lifetime and an estimate of the chemical shift difference between sites. According to the two-site model,

$$1/T_{1\rho}(\text{exch}) = p_A p_B \Delta\omega^2 \frac{\tau_{\text{exch}}}{1 + (\omega_1 \tau_{\text{exch}})^2} \qquad (1)$$

where p_A and p_B are the equilibrium probabilities at the sites, $\Delta\omega$ is the chemical shift difference between the sites, ω_1 is the precession frequency about the spin-locking field, and τ_{exch} is the exchange lifetime and equals $1/(k_{AB} + k_{BA})$. Values for τ_{exch} and $\Delta\omega$ may be extracted from a plot of $T_{1\rho}$(exch) against ω_1^2. τ_{exch} is independent of the $p_A p_B$ product. A minimum value for $\Delta\omega$ is obtained if equal populations are assumed. Although a two-site model is not realistic for conformation exchange in a peptide of any complexity, it can provide indications of characteristic times for conformational exchange. A study of this type was reported by Bleich et al.[3] for the tyrosine ring protons of methionine enkephalin. That work concerned carbon-bound protons and rotational reorientation sufficiently fast that $1/T_1$(dipole–dipole) = $1/T_{1\rho}$(dipole–dipole). Slower molecular reorientation and direct proton–nitrogen binding in the systems described here require more complex analysis to extract the exchange contribution.

Earlier, we reported significant differences in the chemical exchange contributions to $1/T_{1\rho}$ for the peptide bond protons of a pair of diastereomeric cyclic octapeptides, cyclo(D-Ala-Gly-Pro-Phe)$_2$ and cyclo(D-Ala-Gly-Pro-D-Phe)$_2$.[4] The differences were taken to support other indications of greater conformational mobility for the D-Ala, L-Phe isomer. Measurements were made only at ambient temperature. We have now examined at variable temperature rotating frame relaxation of cyclo(Cys-Gly-Pro-Phe)$_2$ (I), in which motions of the cyclic peptide backbone are inhibited by a transannular disulfide bridge, and cyclo(Ala-Gly-Pro-Phe)$_2$ (II),[5] the unbridged analogue of the same stereochemistry. The preparation and a crystal structure of I are also reported here.

Exchange contributions to amide proton $T_{1\rho}$ relaxation were measured as a function of temperature and H_1 field strength. In the 15–55 °C temperature range chemical exchange processes affecting $T_{1\rho}$ in I were found to include at least two components, one clearly temperature dependent and the other with much smaller, if any, temperature dependence. For II no clear temperature dependence was found between 0 and 45 °C. We have tentatively assigned modes of conformational motion involved in

* Illinois Institute of Technology. Present address: L-940, Smith Kline & French Laboratories, P.O. Box 1539, King of Prussia, PA 19406.
† Illinois Institute of Technology. ‡ Roswell Park Memorial Institute.

(1) Deverell, C.; Morgan, R. E.; Strange, J. H. *Mol. Phys.* **1970**, *18*, 553–559.
(2) Bleich, H. E.; Glasel, J. A. *Biopolymers* **1978**, *17*, 2445–2457.
(3) Bleich, H. E.; Day, A. R.; Freer, R. J.; Glasel, J. A. *Biochem. Biophys. Res. Commun.* **1979**, *87*, 1146–1153.
(4) Kopple, K. D.; Bhandary, K. K.; Kartha, G.; Wang, Y.-S.; Parameswaran, K. N. *J. Am. Chem. Soc.* **1986**, *108*, 4637–4642.
(5) Kopple, K. D.; Parameswaran, K. N.; Yonan, J. P. *J. Am. Chem. Soc.* **1984**, *106*, 7212–7217.

0002-7863/88/1510-4168$01.50/0

I, basing the assignment on indications from the crystal structure of I, on the comparison of $T_{1\rho}$ data from I and II, and on differential line broadening effects observed in spectra measured at lower temperatures.

Experimental Procedures

Synthesis. Boc-Cys(Acm)-Gly-Pro-Phe-OMe was synthesized by stepwise coupling of Cbz-Pro-ONSu, Cbz-Gly-ONSu, and Boc-Cys-(Acm)-ONSu to H-Phe-OMe. The Cys active ester, prepared according to Veber et al.,[6] failed to crystallize and was used as an oil. Half of this blocked tetrapeptide was converted to hydrazide by treatment with excess hydrazine in concentrated methanolic solution, and the other half was N-deblocked by treatment with hydrogen chloride in ethyl acetate. The two tetrapeptide fragments were coupled in dimethylformamide by the azide procedure. Blocked intermediates to this stage were isolated free of impurities on thin-layer chromatographic analysis, but they were not crystallized.

Boc-(Cys(Acm)-Gly-Pro-Phe)$_2$-NHNH$_2$. The blocked octapeptide methyl ester (3.66 g, 3.38 mmol) was dissolved in 10 mL of absolute methanol, 3.2 g (30 equiv) of 95% hydrazine was added, and the solution was stored at room temperature overnight. Concentration under reduced pressure gave an oil that crystallized on addition of ethyl acetate to give 3.3 g (90%) of pure hydrazide, mp 154–157 °C dec. An analytical sample was dried for 48 h at 100 °C under vacuum. For $C_{49}H_{70}N_{12}O_{12}S_2 \cdot 1.5H_2O$, C, H, N, S.

Cyclo(Cys(Acm)-Gly-Pro-Phe)$_2$. The Boc-octapeptide hydrazide (1.7 g, 1.52 mmol) was suspended in 60 mL of ethyl acetate, and the mixture was saturated with anhydrous hydrogen chloride (10 min) and flushed with dry nitrogen (20 min). The resulting octapeptide hydrazide hydrochloride was collected by filtration and stored overnight under vacuum over KOH pellets. This product was dissolved in 8 mL of dimethylformamide and held at −25 °C while 3.7 mL of freshly prepared 2.45 M hydrogen chloride in tetrahydrofuran (−25 °C) was added, followed by 0.31 mL (1.5 equiv) of isoamyl nitrite. After 30 min at −25 °C the reaction mixture gave a negative spot test for hydrazide. It was chilled to −60 °C and mixed with 500 mL of dimethylformamide at −60 °C. *N*-Methylmorpholine (1.34 mL, 8 equiv) was added, and the solution was allowed to warm to −15 °C. Additional base was added to maintain the pH at 8, as determined by a probe on moistened indicator paper. After 3 days at −15 °C the solvent was removed under vacuum and the residue was dissolved in water and repeatedly extracted with ethyl acetate. The residue on evaporation of the ethyl acetate was twice precipitated from ethanol by ethyl acetate to give 870 mg (62%) of cyclic octapeptide. An analytical sample was crystallized from 1-butanol and dried 2 days under vacuum at 100 °C, mp 215–218 °C dec. For $C_{44}H_{58}N_{10}O_{10}S_2 \cdot 2H_2O$ C, H, N, S. M + H = 951, M + Na = 973.

Cyclo(CysGly-Pro-Phe)$_2$. The Acm derivative was oxidized directly to the disulfide according to Kamber.[7] To the *S*-acetamidomethyl cyclic peptide (48 mg, 0.05 mmol) in 350 mL of 15% aqueous methanol at room temperature was added 50 mL of 1 mM iodine (13 mg of I_2) in methanol, dropwise with stirring over 1 h. The red solution was cooled to 0 °C and titrated with 1 M aqueous sodium thiosulfate to remove the color. A 50% excess of thiosulfate was added. The methanol was removed under vacuum and as the solution was concentrated 34 mg of disulfide-bridged peptide precipitated. Recrystallization from ethanol afforded 25 mg (62%), mp 288–290 °C dec. The analytical sample was dried 2 days at 100 °C under vacuum. For $C_{38}H_{46}N_8O_8S_2 \cdot 0.5H_2O$, C, H, N, S. M + H = 807.

X-ray Analysis. Crystals of cyclo(Cys-Gly-Pro-Phe)$_2$ were grown by slow evaporation of a solution of the octapeptide in methanol. A crystal measuring 0.25 × 0.30 × 0.70 mm, mounted in a capillary with mother liquor, was used for cell dimension determination and intensity data collection. Unit cell constants were determined by least-squares fit of 25 well-centered reflections. Cyclo(Cys-Gly-Pro-Phe)$_2$ crystallizes in the monoclinic unit cell of dimensions a = 10.164 (6) Å, b = 13.610 (1) Å, c = 15.702 (3) Å, and β = 101.12 (3)°, volume 2131 Å^3, space group $P2_1$. There are two formula units, $C_{38}H_{46}N_8O_8S_2 \cdot 4H_2O$, in the unit cell, with a calculated density of 1.370 g/cm^3.

Intensity data to 2θ = 154° were collected with an Enraf-Nonius CAD-4 automatic diffractometer with use of Cu Kα (λ = 1.5418 Å) radiation. A total of 4697 unique reflections were measured using the $\omega - 2\theta$ scan technique. Three reflections measured every 2 h showed a loss in intensity of about 15% at the end of data collection. Intensity data were corrected for this loss with use of the program DECAY, which is a part of the Structure Determination Package.[8] Intensities were also corrected for Lorentz and polarization effects, and an empirical absorption correction[9] was also applied. (Minimum and maximum corrections were 0.9653 and 0.9986, respectively.)

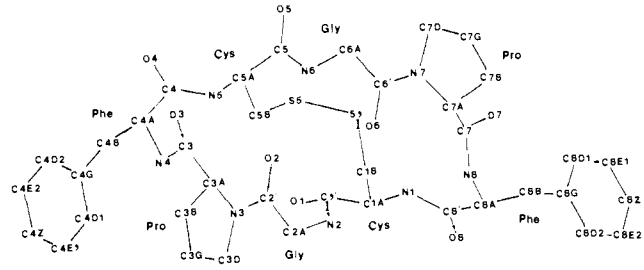

Figure 1. Numbering scheme used for cyclo(Cys-Gly-Pro-Phe)$_2$.

The structure was determined by a combination of the Patterson technique and MULTAN.[10] Coordinates of the two sulfur atoms could be determined from a Patterson map. The structure was developed by successive weighted Fourier maps by using the sulfur atom positions initially and adding the fragments obtained at each step. All but three atoms of a phenyl ring were obtained. A difference Fourier map computed after a few cycles of least-squares refinement revealed the positions of the three atoms of the phenyl ring in addition to four water molecules. Full-matrix least-squares refinements of the 60 non-hydrogen atoms with isotropic thermal parameters in the initial stages and anisotropic thermal parameters in the final stages were carried out. Hydrogen atoms (31 located from the difference Fourier map, and 22 calculated) were included but not refined. One hydrogen atom of water molecule OW3 could not be located. The final R factor for 3654 reflections considered observed ($I > 2\sigma(I)$) was 0.044 (Rw = 0.055 and for all 4697 reflections the R = 0.069). The final shift/error was 0.01 and the goodness-of-fit parameter was 3.38. All the calculations were carried out using the Structure Determination Package[8] with a PDP 11/34 computer system.

NMR Measurements. NMR spectra and relaxation data were obtained on a Nicolet NT-300 spectrometer as described previously.[4] To obtain relaxation data below the freezing point of dimethyl sulfoxide, relaxation measurements were made using solutions in 1:1 (v/v) Me_2SO-d_6–$CDCl_3$. Spectra of cyclo(Cys-Gly-Pro-Phe)$_2$ and cyclo(Ala-Gly-Pro-Phe)$_2$ are not significantly different in this mixture from spectra of solutions in Me_2SO-d_6 alone. Samples were degassed and sealed, and a single sealed sample of each peptide was used for all proton studies. The solutions were used for proton relaxation measurements were 4 mM. Carbon-13 relaxation data were taken from 87 and 54 mM solutions of I and II, respectively. Previous experiments with the D-Ala, D-Phe and D-Ala, L-Phe diastereomers of II had shown no concentration dependence of the ^{13}C T_1 values between 52 and 13 mM.[11]

Proton T_1, carbon T_1, and proton $T_{1\rho}$ relaxation measurements of I were made at 15, 30, 45, and 55 °C. Line broadening precluded measurements below 15 °C. Measurements on II were made at 0, 15, 30, and 45 °C. T_1 was determined by nonselective inversion-recovery, using 9 recovery times between 5 ms and 3 s for carbons and 12 recovery times between 10 ms and 3 s for protons. T_1 values were calculated by using the Nicolet-provided software. $T_{1\rho}$ measurements were made by using spin-locking experiments at 5 or 6 rotating field strengths between 2800 and 8600 Hz. At each transmitter attenuator setting, signal strength was plotted as a function of pulse width in a series of single pulse experiments. Rotating field strengths calculated from the π and 2π pulses agreed within 2%.

For the $T_{1\rho}$ measurements, carrier frequencies were offset from the observed resonances by no more than 100 Hz. Sufficient experiments were carried out at various offsets to establish that offsets up to 200 Hz had no observable effect on the observed rotating frame relaxation for a given NH resonance, even at the lowest rotating field strength. A minimum of 10 spin-locking times between 6 and 600 ms were used. For each temperature and field strength the contribution of conformation exchange to the total $T_{1\rho}$ relaxation rate was estimated as described before.[4] Values of $T_{1\rho}$ (exch) were plotted against ω^2, to obtain from eq

(6) Veber, D. F.; Milkowski, J. D.; Varga, S. L.; Denkewalter, R. G.; Hirschmann, R. *J. Am. Chem. Soc.* **1972**, *94*, 5456–5461.
(7) Kamber, B. *Helv. Chim. Acta* **1971**, *54*, 927–930.
(8) Structure Determination Package, A system of computer programs, Frenz, B. A. & Associates Inc., College Station, Texas, and Enraf-Nonius, Delft, Holland, 1986.
(9) North, A. C. T.; Phillips, D. C.; Mathews, F. C. *Acta Crystallogr.* **1968**, *A24*, 351–359.
(10) Main, P.; Hull, S. E.; Lessinger, L.; Germain, G.; Declerq, J.-P.; Woolfson, M. M., MULTAN 80, A System of Computer Programs for the Automatic Solution of Crystal Structures from X-ray Diffraction Data. Universities of York and Louvain: York, England, and Louvain, Belgium, 1980.
(11) Wang, Yu-Sen Ph.D. Thesis, Illinois Institute of Technology, 1987.

Table I. Bond Distances (Å) and Angles (deg) in Cyclo(Cys-Gly-Pro-Phe-Cys-Gly-Pro-Phe)

	Cys	Gly	Pro	Phe	Cys	Gly	Pro	Phe
i =	1	2	3	4	5	6	7	8
			(a) Bond Distances[a]					
Ni–CiA	1.459	1.434	1.468	1.453	1.445	1.446	1.460	1.457
CiA–Ci′	1.525	1.514	1.508	1.511	1.528	1.510	1.508	1.507
Ci′–Oi	1.248	1.235	1.230	1.237	1.220	1.242	1.234	1.231
Ci′–Ni+1	1.325	1.350	1.336	1.337	1.339	1.333	1.334	1.337
CiA–CiB	1.548		1.511	1.546	1.518		1.524	1.536
CiB–CiG			1.389*	1.492			1.514	1.497
CiG–CiD			1.479*				1.517	
CiD–Ni			1.474				1.456	
CiB–Si	1.824				1.824			
CiG–CiD1				1.365				1.400
CiD1–CiE1				1.392				1.371
CiE1–CiZ				1.343				1.346
CiZ–CiE2				1.376				1.368
CiE2–CiD2				1.379				1.374
CiD2–CiG				1.386				1.366
S1–S5	2.026				2.026			
			(b) Bond Angles[a]					
Ci–1′–Ni–CiA	121.5	122.6	121.2	121.2	123.4	121.3	119.4	124.0
Ni–CiA–Ci′	113.0	113.0	116.0	113.7	112.8	108.3	110.3	113.6
CiB–CiA–Ni	113.3		104.1	109.9	107.1		103.2	114.1
CiB–CiA–Ci′	113.4		111.9	108.4	112.5		113.5	113.0
CiA–Ci′–Oi	118.1	122.8	118.6	119.1	121.1	120.7	121.3	118.8
CiA–Ci′–Ni+1	118.9	115.7	118.0	117.4	116.4	117.8	116.0	119.5
Oi–Ci′–Ni+1	122.7	121.7	123.2	123.5	122.6	121.5	122.7	121.6
Ci–1′–Ni–CiD			126.0				127.0	
CiA–Ni–CiD			112.1				113.6	
CiA–CiB–CiG			108.0*	111.7			103.9	111.7
CiB–CiG–CiD			113.1*				104.6	
CiG–CiD–Ni			102.3				101.9	
CiB–CiG–CiD1				120.9				120.5
CiB–CiG–CiD2				121.3				121.7
CiD1–CiG–CiD2				117.8				117.7
CiG–CiD1–CiE1				121.1				120.3
CiD1–CiE1–CiZ				120.4				120.6
CiE1–CiZ–CiE2				119.8				120.3
CiZ–CiE2–CiD2				119.8				119.7
CiE2–CiD2–CiG				121.0				121.4
CiA–CiB–Si	114.5				115.0			
C1B–S1–S5	103.8							
S1–S5–C5B					104.9			

[a] Average esd in bond distances and angles are 0.007 Å and 0.6°, respectively. Values indicated by an asterisk are affected by the high thermal vibrations of CB and CG atoms of Pro[3].

Table II. Torsional Angles (deg) for Cyclo(Cys-Gly-Pro-Phe-Cys-Gly-Pro-Phe)[a]

		Cys	Gly	Pro	Phe	Cys	Gly	Pro	Phe
	i =	1	2	3	4	5	6	7	8
main chain									
Ci–1′–Ni–CiA–Ci′	ϕ	−133.7	102.0	−62.7	−96.2	−125.9	157.2	−53.0	74.3
Ni–CiA–Ci′–Ni+1	ψ	11.1	172.9	−22.7	0.6	−59.7	170.9	136.9	0.9
CiA–Ci′–Ni+1–Ci+1A	ω	165.1	−167.8	−179.2	−163.1	−174.4	176.7	178.0	171.8
Pro/Phe									
CiD–Ni–CiA–CiB	χ^0			2.8				5.2	
Ni–CiA–CiB–CiG	χ^1			1.2	−54.5			−25.2	−60.6
CiA–CiB–CiG–CiD	χ^2			−4.7	104.0			36.1	−87.9
CiB–CiG–CiD–Ni	χ^3			6.2				−32.0	
disulfide bridge									
N1–C1A–C1B–S1	χ^2	59.2							
C1A–C1B–S1–S5	χ^2	117.2							
C1B–S1–S5–C5B	χ^{33}	−89.3							
S1–S5–C5B–C5A	χ^2	−98.5							
S5–C5B–C5A–N5	χ^1	177.4							

[a] Average esd in torsion angles is 0.7°.

1 the effective values of τ_{exch} and $\Delta\omega$ by least-squares analysis.

$T_{1\rho}$ measurements of I at 15 °C were repeated three times at each of 6 rotating field strengths. A standard deviation of 3 ms was established for $T_{1\rho}$ measurements from these data. This and the comparable standard deviations from the ^1H and ^{13}C T_1 measurements at each temperature were propagated through the calculations to give estimated errors of ±7–8% in $T_{1\rho}$(exch). Less systematic repetitions at other temperatures indicated the same experimental errors.

Results

Crystal Structure. Figure 1 shows the atom numbering scheme used. The final atomic positions and equivalent isotropic thermal parameters are provided as Supplementary Material. Bond lengths and angles are listed in Table I and torsional angles are given in Table II. The average estimated standard deviations in bond lengths, angles, and torsion angles are .007 Å, 0.6°, and 0.7°,

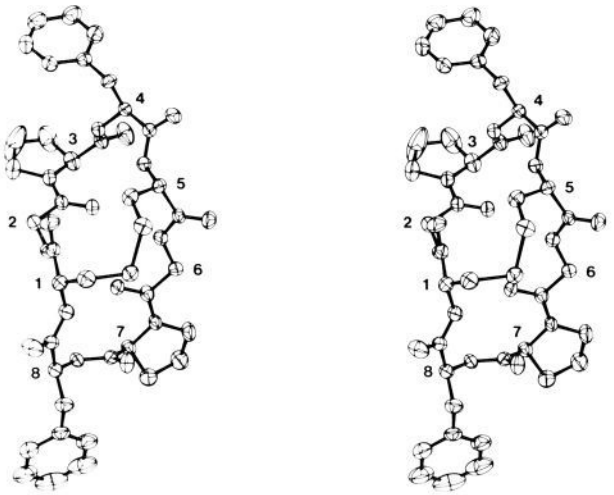

Figure 2. Stereoview of the structure of cyclo(Cys-Gly-Pro-Phe)$_2$ determined by X-ray crystallographic analysis.

respectively. Bond lengths and angles agree well with those reported for cyclic[12] and linear[13] peptides. Although minor differences in equivalent bond lengths in the two halves occur, only the differences in the bond lengths C′–O and C_α–C_β in the Cys residues are above the 3σ level and can be considered significant.

A stereoview of the conformation of the octapeptide is shown in Figure 2. The backbone is similar to backbones found for cyclo(D-Ala-Gly-Pro-D-Phe)$_2$[14] and cyclo(D-Ala-Gly-Pro-Phe)$_2$,[4] in that two roughly planar halves formed by Pro-Phe β-turns form a dihedral. The angle between the two "best planes" through the α-carbons of Cys^1-Gly^2-Pro^3-Phe^4-Cys^5 and Cys^5-Gly^6-Pro^7-Phe^8-Cys^1 is 81°, close to that found earlier for cyclo(D-Ala-Gly-Pro-D-Phe)$_2$, although in the opposite sense. The disulfide bridge is on the convex side of the bend. All of the peptide links are trans; ω of Cys^1, Gly^2, and Phe^4 depart by 15°, 12°, and 17°, respectively, from 180°; the values for all of the others are within 6° of 180°. Although there is C_2 sequence symmetry, the backbone conformation is asymmetric, with major differences in the torsional angles around the Cys-Gly links and the Pro-Phe links in the two halves of the octapeptide (refer to ψ_{Cys}, ϕ_{Gly} and ψ_{Pro}, ϕ_{Phe} in Table II). Relative to the α-carbon framework, the orientations of the two Cys-Gly peptide bond planes differ by about 60°. The orientations of the Pro-Phe peptide planes of the β-turns, relative to their local α-carbon planes, differ by 160–170°; there are a type I β-turn at Gly^2-Pro^3-Phe^4-Cys^5 and a type II turn at Gly^6-Pro^7-Phe^8-Cys^1. Both turns have dihedral angles close to the standard Venkatachalam[15] values and include 4 → 1 hydrogen bonds.

Type II β-turns with α-substituted residues of like configuration at $i + 1$ and $i + 2$, as at Pro^7-Phe^8, are of intrinsically higher energy than type I turns, but they have been observed in peptide crystals before. Examples in the literature are Pro-Ala in isobutyryl-Pro-Ala-isopropylamide,[16] Phe-Ala in two differently solvated molecules of cyclo(Pro-Val-Phe-Phe-Ala-Gly)$_2$,[17] and Phe-Gln in pressinoic acid.[18] Intermolecular hydrogen bonding may contribute to the stability of the type II form in the first two examples. In pressinoic acid, the N—H and the C=O of the Phe-Gln link are involved in intramolecular hydrogen bonds. In crystals of cyclo(Cys-Gly-Pro-Phe)$_2$ the type II turn may derive stabilization from the hydrogen bond between Phe^8 N—H and the Cys^5 C=O of an adjacent molecule (see below). However, in solution the type II turn is less probable, as discussed with the NMR observations.

The disulfide bridge of cyclo(Cys-Gly-Pro-Phe)$_2$ is also not symmetrical. χ^1 for Cys^1 and Cys^5 are near 60° and 180°, respectively, and the χ^2 values are near 120° and −100°. The C–S–S–C torsion is left handed.

The octapeptide backbone of cyclo(Cys-Gly-Pro-Phe)$_2$ is strikingly similar to that of β-amanitin,[19,20] even though the transannular bridges in the two peptides differ (CH_2–S–S–CH_2 and CH_2–S(O)–C_{Aryl}–C_{Aryl}–CH_2). With the residue alignment

Cys^1-Gly^2-Pro^3- - -Phe^4- - -Cys^5-Gly^6-Pro^7-Phe^8 (I)

Cys- -Asp- -Hyp- -DiHyIle-HyTrp-Gly- -Ile- -Gly
(β-amanitin)

Table III. Hydrogen Bonding and Short Contact Distances below 3.2 Å in Cyclo(Cys-Gly-Pro-Phe)$_2$·4H$_2$O

atom 1	atom 2	symmetry[a]	distance (esd)
S1	N1	I (0 0 0)	3.252 (4)
S1	N6	I (0 0 0)	3.442 (5)
S1	O6	I (0 0 0)	3.469 (4)
N1	O6	I (0 0 0)	2.937 (5)
O1	OW2	II (0 −1 0)	2.973 (6)
N2	O6	I (0 0 0)	3.135 (5)
N2	OW3	I (−1 0 0)	2.885 (5)
O2	N4	I (0 0 0)	3.048 (5)
O2	N5	I (0 0 0)	2.990 (5)
O2	N6	I (0 0 0)	3.108 (6)
O3	OW1	II (1 −1 1)	2.860 (5)
N4	OW2	II (0 −1 0)	3.053 (5)
O4	OW3	I (0 0 0)	2.835 (6)
O5	N8	I (1 0 0)	2.998 (5)
O5	OW1	I (0 0 0)	2.822 (5)
O6	O7	I (0 0 0)	3.154 (5)
O6	OW3	I (−1 0 0)	3.142 (6)
O7	OW4	I (0 0 0)	2.767 (6)
O8	OW2	I (0 0 0)	2.798 (5)
OW1	OW4	II (1 −1 1)	2.785 (7)
OW3	OW4	II (1 −1 1)	2.805 (7)

[a] Symmetry: I, x, y, z; II, $-x$, $^1/_2 + y$, $-z$.

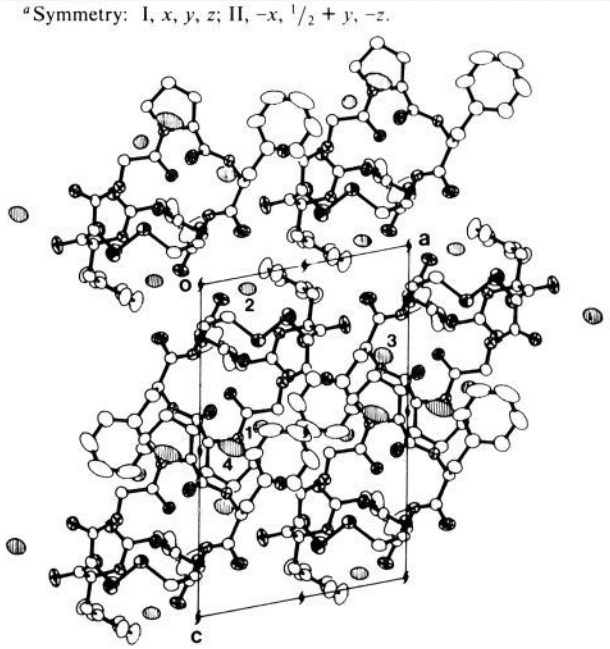

Figure 3. Crystal packing of cyclo(Cys-Gly-Pro-Phe)$_2$·4H$_2$O viewed down the *b* axis.

(12) Karle, I. L. In *Peptides*; Proceedings of the 6th American Peptide Symposium; Gross, E., Meienhofer, J., Eds.; Pierce Chemical Co.: Rockford, IL, 1979; pp 681–690.
(13) Benedetti, E. In *Peptides*, Proceedings of the 5th American Peptide Symposium; Goodman, M., Meienhofer, J., Eds.; Wiley: New York, 1977; pp 257–273.
(14) Kopple, K. D.; Kartha, G.; Bhandary, K. K.; Romanowska, K. *J. Am. Chem. Soc.* **1985**, *107*, 4893–4897.
(15) Venkatachalam, C. M. *Biopolymers* **1968**, *6*, 1425–1436.
(16) Aubry, A.; Protas, J.; Boussard, G.; Marraud, M. *Acta Crystallogr.* **1977**, *B33*, 2399–2406.
(17) Karle, I. L.; Chiang, C. C. *Acta Crystallogr.* **1984**, *C40*, 1381–1386.
(18) Langs, D. A.; Smith, G. D.; Stezowski, J. J.; Hughes, R. E. *Science* **1986**, *232*, 1240–1232.
(19) Kostansek, E. C.; Lipscomb, W. N.; Yocum, R. R.; Thiessen, W. E. *Biochemistry* **1978**, *18*, 3790–3795.
(20) Shoham, G.; Rees, D. C.; Lipscomb, W. N.; Zanotti, G.; Wieland, T. H. *J. Am. Chem. Soc.* **1984**, *106*, 4606–4615.

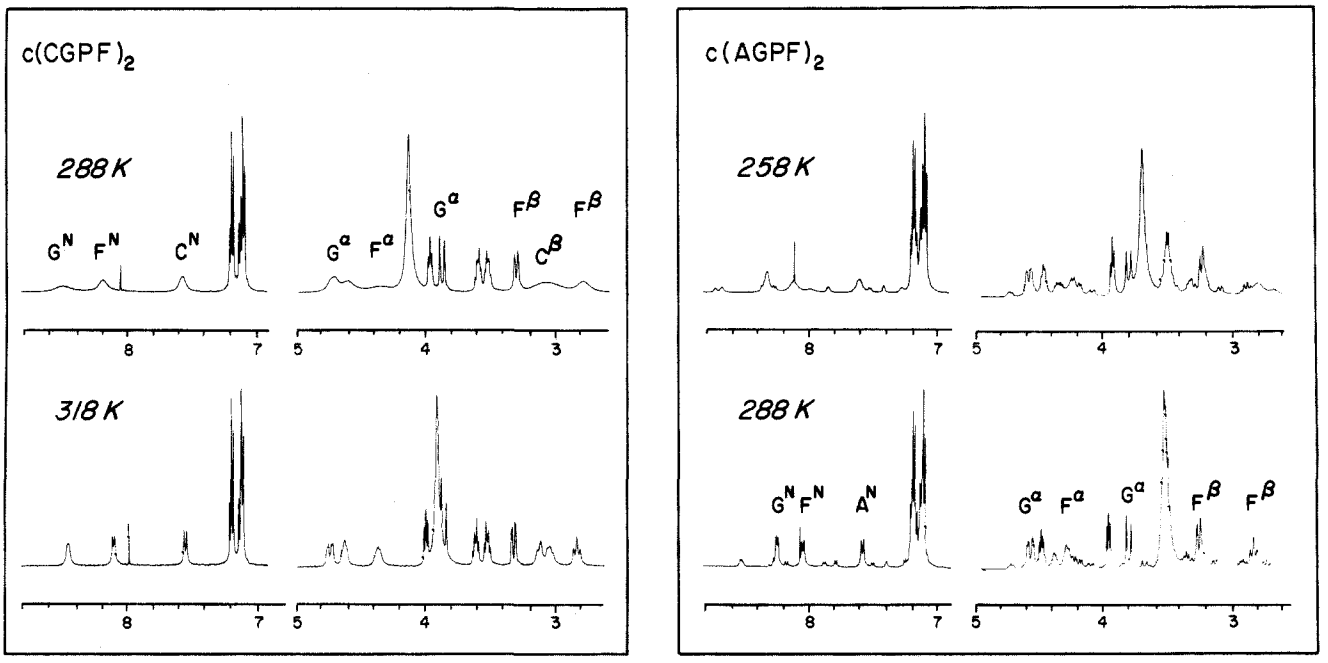

Figure 4. Proton NMR spectra at 500 MHz of cyclo(Cys-Gly-Pro-Phe)$_2$ at 15 and 45 °C (left) and of cyclo(Ala-Gly-Pro-Phe)$_2$ at −15 and 15 °C (right); solvent is 1:1 DMSO-d_6–$CDCl_3$. Resonances referred to in the text are labeled. The minor components in cyclo(Ala-Gly-Pro-Phe)$_2$ have cis Gly-Pro bonds.

the corresponding backbone dihedral angles of I and β-amanitin agree within 22° or less except for one pair: ψ_{Cys} and ϕ_{Asp} differ from ψ^1_{Cys} and ϕ^2_{Gly} in a manner corresponding to a 90° rotation of the plane of the Cys-Asp peptide bond.

Another structure similar to that found for cyclo(Cys-Gly-Pro-Phe)$_2$ is that of the disulfide bridged octadepsipeptide des-*N*-tetramethyltriostin A, which has the backbone sequence (Acyl-D-Ser-Ala-Cys-Val)$_2$, a 26- rather than 24-atom ring.[21] In the crystal the backbone of this molecule can also be described as comprising two planes forming a dihedral at the Cys α-carbons. Here the disulfide bridge is characterized by χ^1, χ^2 (Cys) angles near −60°, −90°, and a right-handed C–S–S–C torsion.

For the cyclo(Cys-Gly-Pro-Phe)$_2$ crystal, possible hydrogen bonding interactions below 3.2 Å and other short contacts are given in Table III. The crystal packing viewed down the *b* axis is shown in Figure 3. All of the carbonyl oxygens and amide N–H units are involved in hydrogen bonds, and all 4 water molecules in the asymmetric unit form good hydrogen bonds with the octapeptide. One interpeptide hydrogen bond ($r_{O\cdots N}$ = 3.0 Å, $r_{O\cdots H}$ = 2.2 Å) is formed between the carbonyl oxygen of Cys^5 and the Phe^8 amide N–H of a symmetry related molecule.

Proton Magnetic Resonance Spectra. The proton and carbon magnetic resonance spectra of cyclo(Cys-Gly-Pro-Phe)$_2$ at 55 °C show the peptide to be C_2 symmetric in the chemical shift time average. Table IV shows that the conformationally relevant observables are like those for cyclo(Ala-Gly-Pro-Phe)$_2$ in its dominant, all peptide bonds trans, form. Parallels in the relative chemical shifts and temperature dependences of the N–H proton resonances, in the backbone H–N–C–H coupling constants, in the large chemical shift difference between the Gly α-protons, and in the chemical shifts of the Pro β- and γ-carbons all indicate that the average backbone conformation of the two peptides is similar. The Phe and Pro β-proton data indicate also that the conformational distribution of the Phe side chains is similar in the two peptides.

The two peptides differ in that spectra of cyclo(Cys-Gly-Pro-Phe)$_2$ are exchange broadened at 45 °C and below, while line broadening in cyclo(Ala-Gly-Pro-Phe)$_2$ is only apparent below 0 °C. Figure 4 compares the 500-MHz proton spectra of I at 45 and 15 °C and II at 15 and −15 °C. Greatest broadening in the proton spectra of I at the lower temperature is seen in the Gly amide, Phe α and Cys β resonances. In addition, the geminal proton pairs of Phe β and Gly α show significant differences, with the lower field Gly α-protons and higher field Phe β-protons being more affected. In the carbon spectra (not shown), the Cys β

Table IV. NMR Data for Cyclo(Cys-Gly-Pro-Phe)$_2$ and Cyclo(Ala-Gly-Pro-Phe)$_2$ in Me_2SO[a]

	cyclo-(Cys-Gly-Pro-Phe)$_2$	cyclo-(Ala-Gly-Pro-Phe)$_2$
	N–H Protons	
Cys, Ala		
δ	7.56	7.62
dδ/dT[b]	−0.0006	−0.001
J_{NHCH}	9.8	8.8
Gly		
δ	8.48	8.20
dδ/dT[b]	−0.0026	−0.003
J_{NHCH}[c]	<2, 7.2	<2, 7.8
Phe		
δ	8.17	8.09
dδ/dT[b]	−0.0013	−0.0026
J_{NHCH}[c]	8.3	8.1
	α-Protons	
$\delta_{Cys,Ala}$	4.62	4.45
δ_{Gly}($J_{\alpha\alpha}$)	4.75 (17.4)	4.51 (17.8)
	3.84	3.87
δ_{Pro}	3.98	3.98
δ_{Phe}	4.36	4.27
	β-Protons	
δ_{Phe} ($J_{\alpha\beta}$)	3.31 (3.3)	3.25 (<5)
	2.80 (12.7)	2.76 (12.2)
δ_{Pro}	1.93, 1.38	1.90, 1.40
	Carbons	
$\delta_{Pro\ \beta}$	28.72[d]	28.52
$\delta_{Pro\ \gamma}$	24.44[d]	24.13

[a] Coupling constant data for the Cys analogue are from spectra at 60 °C because of exchange broadening at lower temperatures. Chemical shift data for the Cys peptide are for 20 °C. [b] Chemical shift temperature coefficient, ppm/deg. Negative coefficients correspond to shift upfield with increasing temperature. [c] Coupling to the higher field α-proton is given first. [d] 30 °C.

(21) Hossain, M. B.; van der Helm, D.; Olson, R. K.; Jones, P. G.; Sheldrick, G. M.; Egert, E.; Kennard, O.; Waring, M. J.; Viswamitra, M. A. *J. Am. Chem. Soc.* **1982**, *104*, 3401–3408.

Table V. Expected and Observed H–N–C–H Coupling Constants (Hz) for Cyclo(Cys-Gly-Pro-Phe)$_2$

	Cys	Gly	Phe
observed[a]	9.8	<2; 7.2	8.3
crystal, calcd[b] (residues 1–4)	>9	4; 8.5	8–8.5
crystal, calcd[b] (residues 5–8)	>9	1.5; 6.5–7	5.5–6
two-site average of crystal	>9	2.7; 7.6	7

[a] Me_2SO, 60°. [b] Calculated using ϕ values of crystal structure, and J_{HNCH} dihedral angle correlation of: Ramachandran, G. N.; Chandrasekaran, R.; Kopple, K. D. *Biopolymers* **1971**, *10*, 2113–2131.

resonance is most broadened, and of the α-carbon resonances, Cys α is the most affected, then Phe α, and Gly α and Pro α least.

Line broadening for the major component of II is less even at considerably lower temperature, and it is qualitatively different. Gly NH is the least, rather than most, broadened NH resonance. The Phe α and the higher field Phe β broaden more than other proton resonances, but the lower field Gly α is much less affected than in I. The Ala β doublet of II is only slightly broadened, in distinct contrast to the Cys β resonance of I.

These evidences of chemical exchange show that single conformations are not dominant in solutions of I and II, even though conformations can be constructed consistent with the averaged NMR observations.

One hypothesis for cyclo(Cys-Gly-Pro-Phe)$_2$ is that the observed spectrum is the average corresponding to fast exchange of the two conformationally distinct halves of the crystal structure. Values of the backbone H–N–C–H coupling constants to be expected for the individual states of this two-site exchange are given in Table V, and their means are compared with observation. Although the observed Cys and Gly H–N–C–H values are not distinguishably different from the expected averages, the Phe H–N–C–H coupling differs significantly from the mean and corresponds to the expectation for a type I rather than type II β-turn. Therefore it is likely that the conformational distribution in solution includes an important fraction of molecules with a more symmetrical (two type I turns) backbone. Coupling constant data for the Cys α–β bond, which might have reported the solution average conformations of the disulfide bridge, are not available from the spectra.

The NMR and crystallographic results thus suggest that two modes of internal motion may be important for cyclo(Cys-Gly-Pro-Phe)$_2$ in solution; they may, however, be coupled. These are rotations of the peptide bond planes relative to the α-carbon framework at Pro-Phe and at Cys-Gly, and reorientations at the Cys side chains. Only the amide plane rotations are possible in cyclo(Ala-Gly-Pro-Phe)$_2$.

Contribution of Conformation Exchange to $T_{1\rho}$ Relaxation. Proton $T_{1\rho}$ relaxation of peptide bond protons was measured at spin-locking fields from 2.6 to 8.6 kHz. Solutions in 1:1 DMSO-d_6–chloroform-d were employed, between 15 and 55 °C for cyclo(Cys-Gly-Pro-Phe)$_2$ and between 0 and 45 °C for cyclo(Ala-Gly-Pro-Phe)$_2$. Attention was focused on the N–H proton resonances, because they are well separated in the spectra and are generally expected to show chemical shifts dependent on conformation. Intermolecular proton exchange is very slow in dimethyl sulfoxide and does not contribute to relaxation in these samples.

The chemical exchange contribution to $1/T_\rho$ was isolated from the total rotating frame T_1 relaxation rate as described earlier.[4] Necessary laboratory frame proton and carbon T_1 relaxation data are reported in Table VI. The C$^\alpha$ relaxation times are near the minima for dipolar relaxation by the directly bonded protons at 75 MHz. However, that the corresponding rotational correlation times are on the extreme narrowing side is unambiguously indicated by the fact that the carbon T_1's decrease as the temperature decreases, and by actual observation of the proton T_1 minima (at 300 MHz) within the temperature ranges studied. At a given temperature the T_1 measurements for the four α-carbon resonances yielded C–H rotational correlation times agreeing within a factor of about 1.5. The only consistent distinction among the values in the 8 sets of measurements was that τ_c was shortest for Gly. However, one effective rotational reorientation time, taken as the mean of the calculated τ_c values for all four individual C–H$^\alpha$ systems, was assumed.

Table VII gives the observed total rotating frame relaxation rates of the peptide N–H protons and the derived exchange contribution $T_{1\rho}$(exch), as measured at each temperature for the lowest and highest spin-locking fields used. Plots of $T_{1\rho}$(exch) versus ω_1^2 gave the straight lines predicted for two-site exchange by eq 1 within the errors estimated for the chemical exchange contribution. The effective exchange lifetimes τ_{exch} and minimum chemical shift differences ($\Delta\nu$) obtained by least-squares analysis are given in Table VIII. Also given is an overall average exchange rate constant calculated assuming an average of the individually obtained N–H lifetimes.

The effective minimum chemical shift differences between the hypothetical two sites are of the magnitude expected for conformation changes in cyclic peptides, 0.5–1 ppm. However, inherent in the results in Table VIII are indications that a two-site model does not describe the internal motions of I or II, even though linear plots of $T_{1\rho}$(exch) versus ω_1^2 were obtained. The chemical shift differences between two well-defined sites should not change with temperature, but the values for II most obviously do. More importantly, although the effective exchange lifetimes for I increase as the temperature goes from 55 to 30 °C, they do not increase further between 30 and 15 °C. This carefully checked behavior indicates that there must be at least two exchange processes with different activation barriers occurring in I. Although $T_{1\rho}$(exch) does not change, many of the resonances continue to broaden as the temperature is reduced below 30 °C, indicating that some exchange process is becoming sufficiently slow at the lower temperatures to contribute to T_2 relaxation. The variation in τ_{exch} for I at the higher temperatures corresponds to a process with an approximately 7 kcal/mol activation barrier. Extrapolation suggests lifetime of the order of 50 μs at 15 °C and 100 μs at 0 °C. Such lifetimes would produce obvious line broadening at 300

Table VI. Laboratory Frame Relaxation Rates ($1/T_1$, s^{-1})

Cyclo(Cys-Gly-Pro-Phe)$_2$

	C$^\alpha$					H^N		
T, °C	Cys	Gly[a]	Pro	Phe	τ_c	Cys	Gly	Phe
15	6.06 (26)	5.62 (6)	6.71 (9)	6.25 (8)	4.54×10^{-10}	3.19 (2)	3.18 (1)	3.47 (2)
30	5.29 (11)	4.90 (2)	5.56 (3)	5.81 (7)	3.42×10^{-10}	3.36 (5)	3.38 (3)	3.61 (7)
45	4.52 (10)	4.23 (4)	4.65 (6)	4.61 (4)	2.55×10^{-10}	3.39 (2)	3.47 (2)	3.60 (3)
55	4.15 (2)	4.07 (8)	4.56 (8)	4.52 (8)	2.41×10^{-10}	3.00 (3)	3.42 (11)	3.28 (2)

Cyclo(Ala-Gly-Pro-Phe)$_2$

	C$^\alpha$					H^N		
T, °C	Ala	Gly[a]	Pro	Phe	τ_c	Ala	Gly	Phe
0	6.75 (14)	5.15 (3)	6.37 (12)	6.21 (4)	4.55×10^{-10}	2.41 (2)	2.32 (2)	2.83 (5)
15	5.88 (31)	4.67 (4)	6.06 (11)	5.43 (32)	3.62×10^{-10}	2.81 (3)	2.75 (2)	3.19 (3)
30	5.00 (8)	3.88 (9)	5.24 (8)	4.83 (14)	2.78×10^{-10}	2.75 (2)	2.91 (5)	3.39 (2)
45	4.24 (11)	3.42 (9)	3.70 (12)	4.15 (7)	2.08×10^{-10}	2.74 (2)	2.69 (1)	3.21 (3)

[a] Values for Gly C$^\alpha$ are $1/2T_{1\ \text{observed}}$

Table VII. Rotating Frame Relaxation Rates ($1/T_{1\rho}$)

Cyclo(Cys-Gly-Pro-Phe)$_2$

		Cys		Gly		Phe	
T, °C	γH_1,[a] Hz	$1/T_{1\rho}$, s^{-1}	$1/T_{1\rho}$(exch), s^{-1}	$1/T_{1\rho}$, s^{-1}	$1/T_{1\rho}$(exch), s^{-1}	$1/T_{1\rho}$, s^{-1}	$1/T_{1\rho}$(exch), s^{-1}
15	2800	10.8	4.8	18.5	12.6	12.8	6.3
	8600	8.4	2.5	10.1	4.2	9.2	2.7
30	2600	10.1	4.9	20.0	14.7	13.0	7.3
	8600	7.8	2.5	10.3	5.0	8.8	3.1
45	2600	8.2	3.6	13.0	8.3	9.4	4.6
	8600	6.9	2.3	9.8	5.1	8.1	3.2
55	3100	7.3	3.4	10.6	6.1	8.3	4.0
	8600	6.5	2.6	9.3	4.8	7.5	3.2

Cyclo(Ala-Gly-Pro-Phe)$_2$

		Ala		Gly		Phe	
T °C	γH_1,[b] Hz	$1/T_{1\rho}$, s^{-1}	$1/T_{1\rho}$(exch), s^{-1}	$1/T_{1\rho}$, s^{-1}	$1/T_{1\rho}$(exch), s^{-1}	$1/T_{1\rho}$, s^{-1}	$1/T_{1\rho}$(exch), s^{-1}
0	3100	11.6	7.3	9.8	5.6	14.3	9.1
	8600	10.2	5.8	9.3	5.2	12.3	7.1
15	3100	9.0	4.5	8.0	3.6	9.8	4.7
	8600	8.1	3.6	7.5	3.1	9.0	3.9
30	3100	7.1	3.3	6.3	2.3	7.6	2.7
	8600	6.4	2.6	6.0	1.9	7.1	2.4
45	3100	6.1	2.7	5.7	2.4	6.2	2.2
	8600	5.5	2.1	5.4	2.1	5.8	1.8

[a] $T_{1\rho}$ was also measured at γH_1 = 4170, 5440, 6940, 7810 Hz. [b] $T_{1\rho}$ was also measured at γH_1 = 4160, 6100, 7690 Hz.

Table VIII. Effective Two-Site Exchange Lifetimes and Minimum Chemical Shift Differences from $T_{1\rho}$ Data[a]

Cyclo(Cys-Gly-Pro-Phe)$_2$

	Cys N–H		Gly N–H		Phe N–H		
T, °C	τ_{exch},[b] μs	$\Delta\nu$,[c] ppm	τ_{exch}, μs	$\Delta\nu$, ppm	τ_{exch}, μs	$\Delta\nu$, ppm	k_{av}[d]
55	11 (1)	0.59 (1)	12 (1)	0.81 (7)	10 (1)	0.68 (5)	4.6×10^4
45	15 (1)	0.54 (2)	16 (1)	0.79 (3)	13 (1)	0.64 (2)	3.4×10^4
30	19 (1)	0.56 (2)	29 (2)	0.81 (3)	24 (1)	0.62 (1)	2.1×10^4
15	20 (1)	0.53 (4)	28 (3)	0.71 (6)	23 (2)	0.56 (4)	2.1×10^4

Cyclo(Ala-Gly-Pro-Phe)$_2$

	Ala N–H		Gly N–H		Phe N–H		
T, °C	τ_{exch}, μs	$\Delta\nu$, ppm	τ_{exch}, μs	$\Delta\nu$, ppm	τ_{exch}, μs	$\Delta\nu$, ppm	k_{av}
45	11 (1)	0.54 (2)	8 (1)	0.59 (3)	9 (1)	0.53 (3)	5.4×10^4
30	10 (1)	0.61 (5)	9 (1)	0.55 (3)	7 (1)	0.64 (2)	5.8×10^4
15	10 (1)	0.73 (1)	8 (1)	0.72 (7)	9 (1)	0.79 (6)	5.6×10^4
0	10 (1)	0.92 (6)	6 (1)[e]	1.01 (15)	10 (1)	1.03 (6)	5.8×10^4

[a] Correlation coefficients for linear plot of $T_{1\rho}$(exch) versus ω_1^2 (6 points for I, 5 for II) is <0.95 except where noted. [b] Exchange lifetime, $1/(k_{AB} + k_{BA})$, for the two-site exchange model. All calculated values rounded to the nearest microsecond. [c] Chemical shift difference between sites for a two-site, equal population exchange model. [d] $k_{av} = 1/2\tau_{av}$, where τ_{av} is over the 3 NH protons at the given temperature. [e] Correlation coefficient 0.91.

MHz for 0.5–1 ppm chemical shift differences between sites. They would also (see Figure 5) result in reduced contributions to $1/T_{1\rho}$(exch) at the higher spin locking fields, which might be compensated for by contributions increasing at the lower temperatures from other, more rapid, motions. Because the 7-kcal/mol process is not observed in II, where Ala residues replace the cystine bridge, and because the line broadening at lower temperatures affects more the Cys and Gly resonances, it seems reasonable that, of the motions suggested by the crystal structure, the 7-kcal/mol process is associated with motional averaging at the $-CH_2-S-S-CH_2-$ bridge and the Cys–Gly peptide bond. If the other motion suggested by the asymmetry of the crystal structure, averaging between type I and II turns at Pro-Phe, were the slow process, the Pro H$^\alpha$ resonance should have been among the more broadened resonances at lower temperatures. This is contrary to observation.

Activation barriers of 7–9 kcal/mol have been reported for acyclic disulfides, e.g., 7.0 kcal/mol for dibenzyl disulfide.[22] Agreement between this value and the value obtained for cyclo(Cys-Gly-Pro-Phe)$_2$ is supportive of the assignment made above, but it must be to a certain extent fortuitous, since disulfide rotation in the peptide must be coupled to other ring motions.

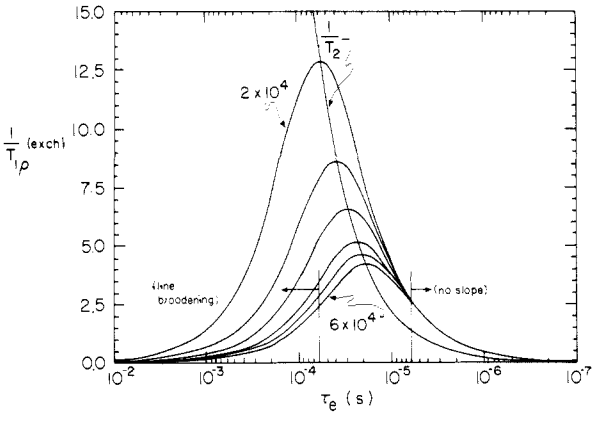

Figure 5. Two-site, equal-probability exchange contribution to rotating frame relaxation (eq 1) for parameters in the range of the present study: chemical shift difference between sites 215 Hz (0.72 ppm at 300 MHz) and rotating field strengths between 2×10^4 (ca. 3200 Hz) and 6×10^4 (ca. 9500 Hz). Also shown is the contribution of the exchange to T_2.

For II, the effective exchange lifetimes from the two-site model are roughly constant over the temperature range in which $T_{1\rho}$ was examined. Considering the errors involved, 2 kcal/mol is a rea-

(22) Fraser, R. R.; Boussard, G.; Saunders, J. K.; Lambert, J. B.; Mixan, C. E. *J. Am. Chem. Soc.* **1971**, *93*, 3822–3823.

sonable estimate of the upper limit for the activation barriers of the process(es) contributing most to $T_{1\rho}$ relaxation in II. The crystal structures for cyclo(D-Ala-Gly-Pro-Phe)$_2$[4] and for cyclo-(Cys-Gly-Pro-Phe)$_2$ suggest that rotations of amide planes relative to the average ring plane, which produce little change in α-carbon positions, are the most likely candidates for the effective motions in II, and for the temperature-independent process in I.

Discussion

Applicability of the Two-Site Model. The two-site exchange model, suitable for cyclohexane,[1] is certainly an oversimplification for cyclic octapeptides. The contribution of multiple site exchange to $T_{1\rho}$ is a sum of terms

$$1/T_\rho(\text{exch}) = \sum_i \Omega_i \frac{\tau_i}{1 + \omega_1^2\tau_i^2} \qquad (2)$$

where the Ω_i are terms with the dimensions of $\Delta\omega^2$, each containing the chemical shift differences between sites and the exchange rate constants, and the τ_i are combinations of the rate constants. Sufficient data to evaluate the unknown rate constants and chemical shift differences will rarely be available. However, to demonstrate what results from the two-site model may represent, we consider a three-site case,

$$A \rightleftharpoons B \rightleftharpoons C$$

with equal populations at the three sites and only two exchange lifetimes, τ_{AB} and τ_{BC}. The required correlation function is obtained following the procedure of Marshall.[23] There are two terms to eq 2, with

$$\tau_\pm = \frac{2\tau_{AB}\tau_{BC}}{\tau_{AB} + \tau_{BC} \pm [\tau_{AB}^2 + \tau_{BC}^2 - \tau_{AB}\tau_{BC}]^{1/2}}$$

If the model is further restricted by assigning chemical shift offsets for the sites as $\omega_A = -\omega_B$ and $\omega_C = 0$ (i.e., carrier on C), the two Ω values are

$$\Omega_+ = \omega_A^2 \frac{\tau_-(4\tau_{BC} - 3\tau_+)}{6\tau_{BC}(\tau_- - \tau_+)} \qquad \Omega_- = \omega_A^2 \frac{\tau_+(3\tau_- - 4\tau_{BC})}{6\tau_{BC}(\tau_- - \tau_+)}$$

For a test case with these restrictions, in which $\omega_A = 600$ rad·s^{-1} (ca. 95 Hz), and $\tau_{AB} = 32$ μs, $\tau_{BC} = 8$ μs, eq 2 becomes

$$1/T_{1\rho}(\text{exch}) = \frac{0.642}{1 + (7.44 \times 10^{-6})\omega_1)^2} + \frac{7.04}{1 + (45.9 \times 10^{-6})\omega_1)^2}$$

When this is computed for $\omega_1 = 1$, 2, 3, 4, and 5×10^4 rad·s^{-1} and the resulting values analyzed on the two-site, equal population model, a straight-line plot with correlation coefficient 0.997 is obtained, yielding τ_{exch}(effective) = 34.5 μs and $\Delta\omega$(effective) = 873 rad·s^{-1}. The results of calculations for other reasonable input values of τ are summarized below (exchange lifetimes in μs, chemical shift differences in rad·s^{-1}).

τ_{AB} ($\Delta\omega$ = 1200 s^{-1})	τ_{BC} ($\Delta\omega$ = 600 s^{-1})	τ_{exch}(eff)	$\Delta\omega$(eff)
32	1	40	840
32	8	34.5	875
16	16	17.6	900
8	32	9.0	915
1	32	$T_{1\rho}$ independent of ω_1	

In each case but the last the correlation coefficient is >0.99. In the last, the ω_1 dependent part of the exchange contribution is <1% of the total. The dominant contribution to τ_{exch}(effective) is from the A = B process, in accord with the expectation that for comparable lifetimes a process with larger $\Delta\omega$ contributes more to the observed relaxation and thus to the apparent lifetime obtained from the two-site model. The calculated $\Delta\omega$ is between the true values, as might also be expected. Thus, in a plausible example, the two-site treatment gives numbers that reflect something of the actual processes.

(23) Marshall, A. G. *J. Chem. Phys.* **1970**, *52*, 2527–2534.

Table IX. Relaxation Rates and Effective Two-Site Exchange Lifetimes and Chemical Shift Differences for Peptide Protons in Four Cyclic Octapeptides[a]

	$1/T_1$, s^{-1}	$1/T_{1\rho}$ (exch), s^{-1}	τ_{exch}, μs	$\Delta\nu$, ppm
cyclo(D-Ala-Gly-Pro-D-Phe)$_2$ (DMSO-d_6, 20 °C)	2.7–3.4	2.9–3.8	<10[b]	*b*
cyclo(D-Ala-Gly-Pro-Phe)$_2$ (DMSO-d_6, 20 °C)	2.9–3.1	5.9–7.5	9–10	0.92–1.07
cyclo(Ala-Gly-Pro-Phe)$_2$ ((DMSO-d_6–$CDCl_3$, 15 °C)	2.8–3.2	3.1–3.8	8–10	0.72–0.79
cyclo(Cys-Gly-Pro-Phe)$_2$ ((DMSO-d_6–$CDCl_3$, 15 °C)	3.2–3.5	2.5–4.2	20–28	0.53–0.71

[a] The range containing results for the three peptide protons is given. $1/T_{1\rho}$ (exch) is for the highest spin locking field used, 8300–8600 Hz. τ_{exch} is $1/(k_{AB} + k_{BA})$ on the two-site exchange model and $\Delta\nu$ is the chemical shift difference for two-site, equal population exchange. [b] Plot of $T_{1\rho}$ versus ω_1^2 has no slope.

The range of exchange rates that give rise to significant contributions to $T_{1\rho}$ is determined by the chemical shift difference between sites. For reasonable differences between peptide conformation exchange sites, say 150 Hz (or 300 Hz) in a 7T static field, eq 1 indicates that exchange contributions to the rotating frame relaxation rate will be less than 1 s^{-1} for lifetimes less than 4 μs (or 1 μs). Use of higher static fields would lower this short lifetime limit. However, at safely accessible rotating field strengths, say 10 kHz (6.3×10^4 rad·s^{-1}), effective exchange lifetimes shorter than 5 μs will not give a detectable dependence of $T_{1\rho}$(exch) on δ_1, so that no estimates for τ_{exch} or $\Delta\omega$ will be obtained. These considerations set a short lifetime limit. On the long lifetime side, for the same chemical shift differences, T_2 broadening may interfere with accurate measurement of $T_{1\rho}$ when τ_{exch} approaches 100 μs. Thus there is a window of observability, illustrated in Figure 5, for motions affecting $T_{1\rho}$. As the temperature is varied, different conformational processes may be made to appear in this window, and insofar as they have different effective chemical shift differences, the apparent effective $\Delta\omega$ may change with temperature, whether or not τ_{exch} changes.

Microsecond Motion in Cyclic Octapeptides. Table IX compares proton spin–lattice (T_1) relaxation rates, the exchange contributions to rotating frame relaxation, the effective conformational exchange lifetimes, and the chemical shift differences for the four cyclic (Xxx-Gly-Pro-Phe)$_2$ peptides we have now examined. The T_1 relaxation rates, which depend on rotational correlation time and interproton distances, and thus on the general size and shape of the peptides, are similar for all four, but the other observations differ among the peptides. The $T_{1\rho}$(exchange) contribution for cyclo(D-Ala-Gly-Pro-D-Phe)$_2$ does not show dependence on the spin locking field strength, but it is comparable in magnitude to the exchange contributions for the other peptides at the highest spin locking fields. According to the discussion above, this indicates a τ_{exch}(effective) in the 1–10 μs range if the chemical shift differences are comparable to those for the other peptides, or else it indicates much smaller chemical shift differences. Either way, this suggests that the D-Ala, D-Phe peptide is the "stiffest" of the octapeptides examined, since it is a reasonable assumption that larger chemical shift differences correlate with greater amplitudes of internal motion. The exchange contributions to $T_{1\rho}$ for cyclo(D-Ala-Gly-Pro-Phe)$_2$ are about twice as large as those for cyclo(Ala-Gly-Pro-Phe)$_2$, although these two diastereomers show about the same effective τ_{exch}. The difference is associated with larger chemical shift differences among sites in cyclo(D-Ala-Gly-Pro-L-Phe)$_2$, suggesting that it is the more flexible molecule. Finally, the disulfide-bridged peptide shows the slowest effective motion, which, as discussed in the Results section, is probably associated more with the disulfide bridge than with amide plane motions that can also occur in the octapeptide backbones.

Summary

In the crystal, cyclo(Cys-Gly-Pro-Phe)$_2$ has an unsymmetrical structure very similar to that of β-amanitin and analogous to other cyclo(Ala-Gly-Pro-Phe)$_2$ diastereomers. In solution to this peptide has internal motion resulting in averaging to apparent C_2 sym-

metry. $T_{1\rho}$ measurements and observation of differential line broadening indicate that this internal motion has at least two components. One, with an approximately 7 kcal/mol activation energy, probably involves the disulfide bridge and adjacent groups. Another motion of much lower barrier probably involves rotation of amide planes relative to the average ring plane, with little change in α-carbon positions. The latter motion is common to other cyclo(Ala-Gly-Pro-Phe)$_2$ analogues.

The exchange contributions to $T_{1\rho}$ relaxation in peptides reflect conformational mobility in the 1-100 μs range. Analysis of these contributions from complex conformation equilibria as though they arise from two-site exchanges gives reasonable indications of conformational lifetimes and site-to-site chemical shift differences.

Acknowledgment. This research was supported by grants from the National Institute of General Medical Sciences, GM 22490 (K.K.B) and GM 26071 (K.D.K.). Mass spectra were obtained by the Midwest Center for Mass Spectrometry at the University of Nebraska, a National Science Foundation Regional Instrumentation Facility (CHE 821164). We are indebted to Dr. Cynthia D'Ambrosio, Smith Kline and French Laboratories, for the 500-MHz spectra shown in Figure 4.

Registry No. BOC-Cys(Acm)-Gly-Pro-Phe-OMe, 114423-77-7; BOC-(Cys(Acm)-Gly-Pro-Phe)$_2$-NHNH$_2$, 114423-78-8; cyclo(Cys-(Acm)-Gly-Pro-Phe)$_2$, 114423-79-9; cyclo(Cys-Gly-Pro-Phe)$_2$, 111967-73-8; cyclo(Cys-Gly-Pro-Phe)$_2$·4H$_2$O, 114423-80-2; Cbz-Pro-ONSu, 3397-33-9; Cbz-Gly-ONSu, 2899-60-7; BOC-Cys(Acm)-ONSu, 19746-38-4; H-Phe-OMe, 2577-90-4; BOC-Cys(Acm)-Gly-Pro-Phe-NHNH$_2$, 114423-81-3; H-Cys(Acm)-Gly-Pro-Phe-OMe·HCl, 114423-82-4; BOC-(Cys(Acm)-Gly-Pro-Phe)$_2$-OMe, 114423-83-5; H-(Cys(Acm)-Gly-Pro-Phe)$_2$-NHNH$_2$·HCl, 114423-84-6; cyclo(Alu-Gly-Pro-Phe)$_2$, 91383-23-2.

Supplementary Material Available: Tables of atomic coordinates and thermal parameters for cyclo(Cys-Gly-Pro-Phe)$_2$·4H$_2$O (6 pages); listing of observed and calculated structure factors (19 pages). Ordering information is given on any current masthead page.

^{1}H NMR Resonance Assignment and Dynamic Analysis of Phenylalanine CD1 in a Low-Spin Ferric Complex of Sperm Whale Myoglobin

S. Donald Emerson, Juliette T. J. Lecomte,† and Gerd N. La Mar*

Contribution from the Department of Chemistry, University of California, Davis, California 95616. *Received September 28, 1987*

Abstract: A proton NMR investigation has been carried out to characterize the dynamic properties of the ring reorientation of the highly conserved phenylalanine CD1 of sperm whale myoglobin. The paramagnetic (Fe(III), $S = {}^1/_2$) met-cyano derivative imparts large chemical shift dispersion that allows detection of the rapid reorientation while retaining relatively narrow lines amenable to unambiguous assignment. The side chain ring peaks for Phe CD1 are assigned on the basis of steady-state and time-dependent nuclear Overhauser effect measurements among the side-chain resonances and between the side-chain resonances and heme resonances in both native and deuterohemin-reconstituted metMbCN and on the basis of differential paramagnetic relaxation. The quantitation of exchange contributions to the line width of the averaged meta H resonances of the ring as a function of temperature yields a ring reorientation rate of $\sim 10^5$ s^{-1} at 25 °C and an activation barrier of 14 ± 4 kcal/mol. This barrier is consistent with a low activation energy process indicative of local concerted structural fluctuations of the C-D helical corner and is inconsistent with global unfolding. The highly conserved nature of the Phe CD1 and its characteristic hyperfine shift that places it in the resolved portion of the ^{1}H NMR spectrum of met-cyano derivatives suggest that the rate of Phe CD1 ring rotation should serve as a useful probe of local dynamic properties of the CD corner in a variety of oxygen-binding heme proteins.

The functional properties of biopolymers are known to be determined not only by their ground-state structure, well described by crystal diffraction methods, but also by their dynamic fluctuations.[1-5] For the oxygen-binding heme proteins myoglobin, (Mb) and hemoglobin (Hb), the biologically important motions range from side-chain rotations that allow oxygen to permeate into the crowded heme pocket[6-8] to large segmental displacements that are involved in cooperativity.[9-11] The remarkable distribution of internal flexibility of biopolymers is illustrated dramatically by the variability of mean-squared displacements measured in the X-ray diffraction experiment for side-chain and backbone atoms in different portions of the Mb molecule.[12-14]

According to static X-ray structures, the packing of most highly folded proteins can be so dense that often the rotation of buried aromatic side chains of phenylalanine (Phe) and tyrosine (Tyr) is quite difficult to envision.[15,16] Yet, early ^{1}H NMR studies have shown that even the most constrained residues exhibit reorientation in the time scale of high-field NMR instruments, $\geq 10^3$ s^{-1}.[17,18] The rotation or flipping of buried Phe and Tyr rings is believed to be permitted by concerted motions often described as transient

† Current address: Department of Chemistry, Pennsylvania State University, Davey Laboratory, University Park, PA 16082.

(1) Gurd, F. N. R.; Rothgeb, T. M. *Adv. Protein Chem.* **1979**, *33*, 73-165.
(2) Karplus, M.; McCammon, J. A. *CRC Crit. Rev. Biochem.* **1981**, *9*, 293-349.
(3) Debrunner, P. G.; Frauenfelder, H. *Annu. Rev. Phys. Chem.* **1982**, *33*, 283-299.
(4) Woodward, C.; Simon, E.; Tuchsen, E. *Mol. Cell. Biochem.* **1982**, *48*, 135-160.
(5) McCammon, J. A. *Rep. Prog. Phys.* **1984**, *47*, 1-84.
(6) Case, D. A.; Karplus, M. *J. Mol. Biol.* **1979**, *132*, 343-368.
(7) Austin, R. H.; Beeson, K. W.; Einstein, L.; Fraunfelder, H.; Gunsallus, R. C. *Biochemistry* **1975**, *14*, 5355.
(8) Perutz, M. F.; Mathews, F. S. *J. Mol. Biol.* **1966**, *21*, 199-202.
(9) Perutz, M. F.; Fermi, G. In *Haemoglobin and Myoglobin Atlas of Molecular Structures in Biology*; Phillips, D. C., Richards, F. M., Eds.; Oxford University: Oxford, 1986; Vol. 2.
(10) Dickerson, R. E.; Geis, R. *Hemoglobin*; Benjamin/Cummings: Menlo Park, CA, 1983.
(11) Gelin, B. R.; Karplus, M. *Proc. Natl. Acad. Sci. U.S.A.* **1977**, *74*(3), 801-805.
(12) Fraunfelder, H.; Petsko, G. A.; Tsernoglou, D. *Nature (London)* **1979**, *280*, 558-563.
(13) Parak, F.; Fink, P.; Mayo, K. H. *Biophys. Struct. Mech.* **1980**, *6*, 51.

0002-7863/88/1510-4176$01.50/0